

TECHNICAL REPORT STANDARD PAGE

| | | | |
|--|--------------------------------------|--|----------------------------|
| 1. Report No. FHWA/LA.0x/xxx | | 2. Government Accession No. | 3. Recipient's Catalog No. |
| 4. Title and Subtitle Use of Steel Fibers for Induction Heating and Self-Healing in Asphalt concrete | | 5. Report Date June 2016 | |
| | | 6. Performing Organization Code LTRC Project Number: 16-5TIRE State Project Number: DOTLT1000092 | |
| 7. Author(s) Mostafa Elseifi, Ph.D., P.E., Yashwanth Pamulapati, Omar S Elbagalati, and Nirmal Dhakal | | 8. Performing Organization Report No. | |
| 9. Performing Organization Name and Address Department of Civil and Environmental Engineering Louisiana State University Baton Rouge, LA 70803 | | 10. Work Unit No. | |
| | | 11. Contract or Grant No. | |
| 12. Sponsoring Agency Name and Address Louisiana Department of Transportation and Development P.O. Box 94245 Baton Rouge, LA 70804-9245 | | 13. Type of Report and Period Covered Final Report July 2015 – June 2016 | |
| | | 14. Sponsoring Agency Code | |
| 15. Supplementary Notes Conducted in Cooperation with the U.S. Department of Transportation, Federal Highway Administration | | | |
| 16. Abstract The objective of this study was to test the hypothesis that a new generation of asphaltic materials could be artificially healed while in-service by embedding metallic fibers in the mix and by applying an electromagnetic field at the surface. To achieve the objective of this study, an open-graded friction course (OGFC) was successfully designed and prepared to incorporate up to 5% steel and aluminum fibers by weight of the mix. The repeatability of the fracture resistance measurements was acceptable with a coefficient of variation ranging from 4.8 to 13.2% with an average of 8.0%. Based on the results of the experimental program, it was found that the control mix and the mix prepared with aluminum fibers exhibited greater ultimate load at failure prior to healing than the specimens with steel fibers. Yet, differences were not statistically significant. After numerous trials, the induction heating experiment was conducted successfully and showed the feasibility of inducing Eddy current in the metallic fibers without contact to the specimens. Eddy current flowed through the metallic fibers and caused heat due to the resistance opposing the current. Given their higher electrical resistivity, the specimens with aluminum required a longer heating time to reach 110°C than the specimens with steel fibers. After the rest period, the control mix had the highest ultimate load after healing although it was not successfully heated through Eddy current; yet, differences were not statistically significant. This indicates that other healing mechanisms were present due to the recovery period, which allowed the control specimens to heal during the rest period. Healing efficiency was the highest for the control specimen as it approached 85%. Healing efficiency for the specimen with aluminum and steel fibers was 72 and 62%, respectively. Microscopic image analysis demonstrated that induced cracks healed efficiently during the healing period. Based on the results of the study, asphalt mixture healing through induction heating was validated and should be further evaluated by the Department through a comprehensive laboratory program. The evaluation of healing through induction heating in field applications should also be considered in future projects especially at the Louisiana Accelerated Loading Facility (ALF). | | | |
| 17. Key Words | | 18. Distribution Statement Unrestricted. This document is available through the National Technical Information Service, Springfield, VA 21161. | |
| 19. Security Classif. (of this report) | 20. Security Classif. (of this page) | 21. No. of Pages 56 | 22. Price |

LTRC Administrator/ Manager

Vijaya Gopu

Directorate Implementation Sponsor

Janice Williams, P.E.

DOTD Chief Engineer

Use of Steel Fibers for Induction Heating and Self-Healing in Asphalt concrete

Mostafa Elseifi, Ph.D., P.E.

Associate Professor

Department of Civil and Environmental Engineering

Louisiana State University

3316r Patrick Taylor Hall

Baton Rouge, LA 70803

e-mail: elseifi@lsu.edu

Yashwanth Pamulapati

Graduate Research Assistant

Omar S Elbagalati

Graduate Research Assistant

Nirmal Dhakal

Graduate Research Assistant

Department of Civil and Environmental Engineering

Louisiana State University

LTRC Project No. 16-5TIRE

State Project No. DOTLT1000092

conducted for

Louisiana Department of Transportation and Development

Louisiana Transportation Research Center

The contents of this report reflect the views of the author/principal investigator who is responsible for the facts and the accuracy of the data presented herein. The contents do not necessarily reflect the views or policies of the Louisiana Department of Transportation and Development or the Louisiana Transportation Research Center. This report does not constitute a standard, specification, or regulation.

June 2016

ABSTRACT

The objective of this study was to test the hypothesis that a new generation of asphaltic materials could be artificially healed while in-service by embedding metallic fibers in the mix and by applying an electromagnetic field at the surface. If successful, self-healing through induction heating will result in a new class of asphaltic materials that is able to resist crack propagation and damage, which is the main failure mechanism in flexible pavements. To achieve the objective of this study, an open-graded friction course (OGFC) was successfully designed and prepared to incorporate up to 5% steel and aluminum fibers by weight of the mix. The repeatability of the fracture resistance measurements was acceptable with a coefficient of variation ranging from 4.8 to 13.2% with an average of 8.0%. Based on the results of the experimental program, it was found that the control mix and the mix prepared with aluminum fibers exhibited greater ultimate load at failure prior to healing than the specimens with steel fibers. Yet, differences were not statistically significant.

After numerous trials, the induction heating experiment was conducted successfully and showed the feasibility of inducing Eddy current in the metallic fibers without contact to the specimens. Eddy current flowed through the metallic fibers and caused heat due to the resistance opposing the current. Induction heating experiments showed that the specimens incorporating metallic fibers reached the target temperature while the control mix did not heat after 35 minutes. Given their higher electrical resistivity, the specimens with aluminum required a longer heating time to reach 110°C than the specimens with steel fibers.

After the rest period, the control mix had the highest ultimate load after healing although it was not successfully heated through Eddy current; yet, differences were not statistically significant. This indicates that other healing mechanisms were present due to the long recovery period, which allowed the control specimen to heal during the rest period. Healing efficiency was the highest for the control specimen as it approached 85%. Healing efficiency for the specimen with aluminum and steel fibers was 72 and 62%, respectively.

Microscopic image analysis demonstrated that induced cracks healed efficiently during the healing period. From the captured images, cracks with width as large as 0.639 mm appeared to have completely closed after the recovery period. The observed healing of the cracks is in agreement with the measured loading capacity of the specimens after the recovery period.

ACKNOWLEDGMENTS

The authors recognize the efforts of Dr. Vijaya Gopu of LTRC, who cooperated with the research team during this project. The Louisiana Department of Transportation and Development (DOTD), Federal Highway Administration (FHWA), and the Louisiana Transportation Research Center (LTRC) financially supported this research project.

IMPLEMENTATION STATEMENT

Based on the results of the study, asphalt mixture healing through induction heating was validated and should be further evaluated by the Department through a comprehensive laboratory program. The evaluation of healing through induction heating in field applications should also be considered in future projects especially at the Louisiana Accelerated Loading Facility (ALF).

TABLE OF CONTENTS

| | |
|---|------|
| ABSTRACT..... | III |
| ACKNOWLEDGMENTS | V |
| IMPLEMENTATION STATEMENT | VII |
| TABLE OF CONTENTS..... | IX |
| LIST OF TABLES..... | XI |
| LIST OF FIGURES | XIII |
| INTRODUCTION | 1 |
| OBJECTIVE | 3 |
| SCOPE | 5 |
| METHODOLOGY | 7 |
| Task 1: Identify and Characterize Steel Fibers Suitable for Use in Asphalt Concrete. | 7 |
| Task 2: Prepare and Characterize Asphalt Concrete Specimens | 8 |
| Task 3: Test and Characterize the Microscopic Properties of the Prepared Blends | 9 |
| Task 4: Stimulate Healing Mechanisms through Induction Heating | 9 |
| Task 5: Prepare Final Report | 10 |
| RESULTS AND ANALYSIS..... | 11 |
| Literature Review..... | 11 |
| Principles of Induction Heating | 13 |
| Applications of Induction Heating to Asphaltic Materials | 14 |
| Healing of Cracks through Induction Heating..... | 19 |
| Laboratory Test Results | 22 |
| Job-Mix Formula | 22 |
| Fracture Resistance of Laboratory Specimens..... | 22 |
| Healing through Induction Heating | 25 |
| Healing Quantification..... | 27 |
| Microscopic Analysis..... | 30 |
| CONCLUSIONS..... | 33 |
| RECOMMENDATIONS..... | 35 |
| ACRONYMS, ABBREVIATIONS, AND SYMBOLS..... | 37 |
| REFERENCES | 39 |

LIST OF TABLES

| | |
|--|----|
| Table 1 Description of the Evaluated Mixes..... | 8 |
| Table 2 Description of the Job Mix Formula..... | 22 |
| Table 3 Fracture Resistance Test Results before Healing | 24 |
| Table 4 Laboratory Induction Heating Time to Reach Target Temperature | 27 |
| Table 5 Fracture Resistance Test Results after Healing | 28 |
| Table 6 Microscopic Images of Cracked Areas after Loading and after the Recovery Period | 31 |

LIST OF FIGURES

| | |
|---|----|
| Figure 1 Processing of steel and aluminum pieces before mix preparation | 7 |
| Figure 2 Distribution of metallic fibers inside a test specimen | 8 |
| Figure 3 Induction-heating healing experiment for cracked test specimens..... | 9 |
| Figure 4 Crack healing process in asphalt concrete [8]..... | 11 |
| Figure 5 Schematic diagram showing five stages of crack healing on opposite surfaces of two random coil chains (a) rearrangement, (b) surface approach, (c) wetting, (d) diffusion to a distance χ , (e) diffusion to a distance χ_{∞} and randomization [9] | 12 |
| Figure 6 Principles of healing through induction heating [16, 17, 18]..... | 15 |
| Figure 7 Maximum reachable temperatures at three different heating times for different volume of fibers [18]..... | 16 |
| Figure 8 Strength recovery ratios at different healing temperatures [17] | 18 |
| Figure 9 Average length of fibers before and after mixing and compacting [18]..... | 19 |
| Figure 10 Electrical conductivity surface of asphalt mastic against the sand-bitumen ratio and the total volume of conductive additives [19] | 21 |
| Figure 11 Typical Test Results from the Fracture Resistance Test for (a) Control and (b) Mix with 5% Steel Fibers | 23 |
| Figure 12 Fracture Resistance Test Results prior to Healing | 25 |
| Figure 13 Thermal Profiles of Laboratory Specimens after 15 minutes for (a) 76CO and (b) 76Fe5.0..... | 26 |
| Figure 14 Fracture Resistance Test Results after Healing | 28 |
| Figure 15 Comparison of the ultimate load before and after the induction heating experiment..... | 29 |
| Figure 16 Calculated Healing Efficiency for the Different Mix Types | 30 |
| after the Recovery Period..... | 31 |
| Figure 17 Measured Crack Widths for the Different Mix Types (before and after Induction Heating)..... | 32 |

INTRODUCTION

One of the major distresses that directly affect the serviceability and quality of flexible pavements is cracking. Cracking appears at the pavement surface as longitudinal cracks, transverse cracks, and a combination of both that extend over the width of the pavement and creates hazardous conditions for the road users. Water infiltration through the cracks may subsequently cause weakening and deterioration of the base and/or subgrade. Cracking is also the main cause of many pavement distresses (e.g., stripping in hot-mix asphalt [HMA] layers, loss of subgrade support, etc.). The rehabilitation of pavement damage caused by cracking failure is usually costly. Therefore, there is a critical need to evaluate and implement emerging technologies, which may enhance the cracking resistance of asphalt concrete.

Healing of asphaltic materials is an intrinsic property that has been reported in the late 1960s and was noticed to occur at high temperatures and with long rest periods between loads [1, 2]. Furthermore, phenomenon such as binder thixotropy allows the time-dependent decrease in viscosity of the binder under shear and the recovery of viscosity when the flow is stopped. Healing was also used to explain the observed differences between laboratory and field fatigue performance [3]. However, the micro-mechanisms responsible for healing were not clearly understood until the healing mechanisms were studied at different length scales in the last two decades [4].

OBJECTIVE

The objective of this study is to test the hypothesis that a new generation of asphaltic materials could be artificially healed while in-service by embedding metallic fibers in the mix and by applying a magnetic field at the surface. If successful, self-healing through induction heating will result in a new class of asphaltic materials that is able to resist cracking propagation and damage, which is the main failure mechanism in flexible pavements.

SCOPE

To achieve the objective of the study, laboratory tests were conducted to validate healing mechanisms through induction heating. Laboratory semi-circular specimens were prepared with varying contents of metallic fibers and were loaded monotonically to failure. Induction heating was then applied on the damaged specimens to stimulate healing mechanisms in the mix. Through induction heating, the proposed self-healing mechanism utilizes the concept of Eddy current and electrically-conductive fibers to generate high temperature inside the composite material. High temperature would then cause asphalt binder to flow and fill the cracks in the material. Healed specimens were then loaded to failure to assess whether part of the load-carrying capacity was recovered. Microscopic analysis was conducted on the laboratory specimens to assess healing of the cracks at the microscopic level.

METHODOLOGY

To achieve the objective of this study, the following five research tasks were conducted.

Task 1: Identify and Characterize Steel Fibers Suitable for Use in Asphalt Concrete

The objective of Task 1 was to explore different types of steel fibers that can be used in the production of self-healing asphalt concrete. To achieve this objective, the research team conducted a literature review and identified available steel fibers' that can be used in the preparation of asphalt concrete specimens. Steel fibers are available in various grades and sizes varying from 0.001 to 0.02 in. In addition to steel fibers, this study evaluated the use of aluminum as an induction heating agent. As necessary, the collected fibers were ground to powder-size that would allow the additive to uniformly blend in the mix, see Figure 1.

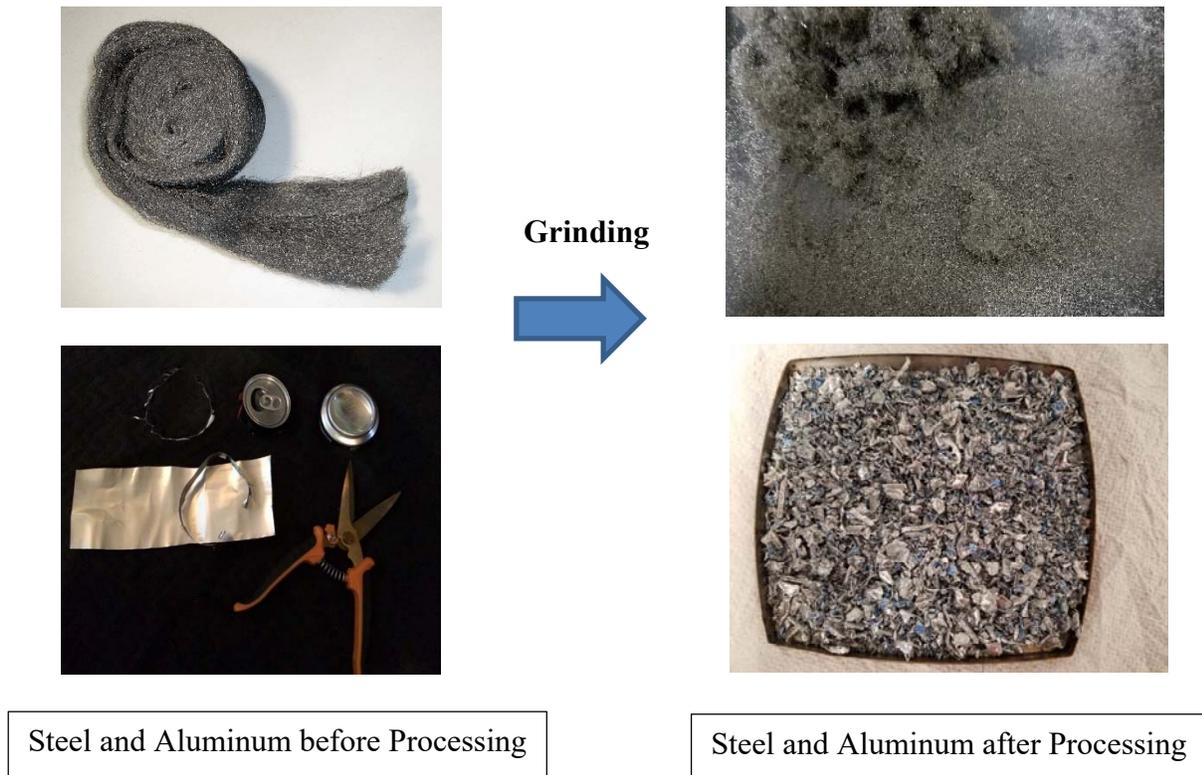


Figure 1
Processing of steel and aluminum pieces before mix preparation

Task 2: Prepare and Characterize Asphalt Concrete Specimens

The objective of this task was to design and to prepare asphalt concrete specimens with varying contents of metallic fibers. A mix design commonly used in Louisiana for open-graded friction course (OGFC) was selected and was modified to incorporate metallic fiber contents of 2.5 and 5.0% by weight of the mix. Table 1 presents the specimens prepared in for this study. It is noted that each mix condition was prepared in duplicate to control variability in the test results. Figure 2 illustrates the distribution of steel fibers inside a test specimen.

Table 1
Description of the Evaluated Mixes

| Mixture ID | Description |
|------------|--|
| 76CO | Conventional OGFC mixture with Polymer-Modified PG 76-22 |
| 76Fe2.5 | OGFC mixture with PG 76-22 and 2.5% steel fibers |
| 76Fe5.0 | OGFC mixture with PG 76-22 and 5% steel fibers |
| 76Al5.0 | OGFC mixture with PG 76-22 and 5.0% aluminum |



Figure 2
Distribution of metallic fibers inside a test specimen

Task 3: Test and Characterize the Microscopic Properties of the Prepared Blends

The objective of this task was to load the prepared specimens until failure and to characterize the microscopic properties of the prepared asphalt concrete specimens in the cracked areas. Cracking potential of the prepared mixtures was assessed using semi-circular unnotched specimens. The semi-circular specimens were loaded monotonically up to the fracture point under a constant cross-head deformation rate of 0.5 mm/min in a three-point bending load configuration. Test temperature was selected to be 25°C. Microscopic analysis was conducted using light microscopy and was used to assess the cracking patterns in the specimen after failure.

Task 4: Stimulate Healing Mechanisms through Induction Heating

The objective of this task was to stimulate and characterize the self-healing capabilities of asphalt concrete test specimens with and without metallic fibers. A specially-designed, single position multi-turn helical coil was built to generate the required heating for the application, see Figure 3a. Initial tests were conducted to optimize the power delivered to the samples in order to reach the desired temperature. The time required to heat the specimen to a temperature of 110°C was monitored.



Figure 3
Induction-heating healing experiment for cracked test specimens

Due to the varying contents of metallic fibers, high content specimens heated relatively quickly as compared to specimens with low to no metallic fibers. The coil was set in horizontal position with one sample set inside of it, resting on a thermo-resistive plate. The temperature of each part of the specimen was monitored throughout the duration of each

experiment using an Infra-Red (IR) camera, see Figure 3b. After heating, the specimens were characterized once more using microscopic analysis and were then loaded to failure to predict the healing efficiency of the prepared mixes and to evaluate whether the specimens recovered part of their fracture resistance through induction heating and other healing mechanisms.

Task 5: Prepare Final Report

A final report was prepared to summarize and document all the findings, experiments, results, conclusions, and challenges encountered during the project period. In addition, recommendations for future research needs was addressed.

RESULTS AND ANALYSIS

Literature Review

Asphalt pavements are prone to cracking due to many factors such as traffic loadings, construction deficiency as well as severe environmental conditions. Cracks are detrimental to pavements in many ways by either weakening its mechanical properties, or lowering its durability by creating pathways for water to enter the structure and accelerate its deterioration and the need for repair. Healing of asphaltic materials is an intrinsic property that has been reported in the late 1960s and was noticed to occur at high temperatures and with long rest periods between loads, see Figure 4 [1, 2]. Healing was also used to explain the observed differences between laboratory and field fatigue performances [3]. However, the micro-mechanisms responsible for healing were not clearly understood until the healing mechanisms were studied at different length scales in the last two decades [4].

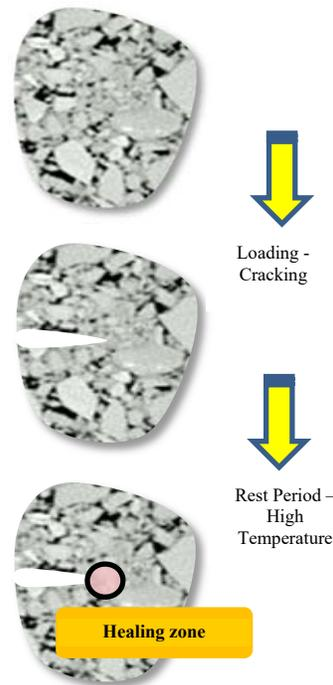


Figure 4
Crack healing process in asphalt concrete [8]

Wool and O'Connor (1981) proposed a theory on crack healing in polymers and stated that healing occurs in five sequential stages namely, surface rearrangement, surface approach, wetting, diffusion, and randomization [9]. A damaged polymer material with known mechanical properties was subjected to healing relating to time (t_h), temperature (T_h), and pressure (P_h). Mechanical properties of the healed material and virgin material was

compared using a dimensionless recovery ratio (R). Figure 5 presents the schematic model showing the five stages of healing on two random-coil chains on opposite crack surfaces. Healing mechanism was described using a domain χ in a crack interface. Wetting distribution function ($\emptyset(t)$) was determined with respect to different types of damages in the polymer material such as cracks, voids, crazes etc. for three different cases, namely, initial wetting, constant rate wetting, and Gaussian wetting. A diffusion initiation function ($\psi(t)$) was introduced to prevent delay of healing rates and the intrinsic healing function $R_h(t)$ equations for fractured stress, strain, and impact energy were derived using a reputation model for healing. In addition, the convolution product of intrinsic healing function and wetting distribution function were used to determine the recovery ratio (R).

Equations affecting the mechanical properties during healing were derived at different conditions of χ such as at $\chi < \chi_\infty$, $\chi = \chi_\infty$ and at χ_∞ (where, $\chi_\infty =$ complete recovery) to support the healing theory. Authors concluded that diffusion stage contributes to the restoration of mechanical properties during healing and the recovery ratios obtained for strength, elongation, impact energy, etc., (which relates the mechanical properties of the material before and after healing) are function of time, temperature, pressure, molecular weight, and processing conditions.

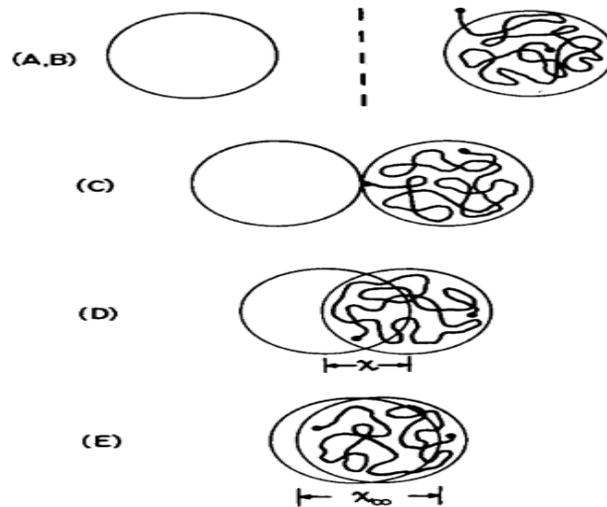


Figure 5

Schematic diagram showing five stages of crack healing on opposite surfaces of two random coil chains (a) rearrangement, (b) surface approach, (c) wetting, (d) diffusion to a distance χ , (e) diffusion to a distance χ_∞ and randomization [9]

Qiu et al. studied the healing properties of asphalt binder using a two-piece healing (TPH) test and the Dynamic Shear Rheometer (DSR) [4]. In this test setup, the crack healing

process was stimulated by pressing two asphalt pieces until the DSR gap was closed. After the gap was closed, the increase in the complex shear modulus during healing time (rest period) was used to quantify healing efficiency of the binder. It was observed that healing occurs in two phases – initial healing phase and time-dependent healing phase. Attempts were also made to describe the healing mechanisms in asphalt binder using a five-stage model that explains the healing process in terms of surface rearrangement, surface approach, wetting, diffusion, and randomization similar to what is observed with thermoplastic polymers [6].

At the macro-level, healing of asphalt concrete was quantified through the increase in stiffness as well as the improvement in fatigue life of the mixture when rest periods are used during laboratory testing [7]. Palvadi et al. studied the fatigue damage and healing characteristics of fine-aggregate mix (FAM) by subjecting laboratory specimens to cyclic torsion and different rest periods [4]. The viscoelastic continuum damage (VECD) theory was used to quantify healing efficiency in FAM mixes as a function of rest periods and damage level. The amount of healing was quantified as the relative reduction in the healing parameter, S, based on the following equation:

$$\% \text{ Healing } (C, t) = \frac{(S_f - S_i)}{S_i} \times 100 \quad (1)$$

where, C is the pseudo stiffness immediately before the rest period, t is the duration of the rest period, S_i is the internal state variable before the rest period, and S_f is the internal state variable after introducing the rest period. It is worth noting that healing can be confounded and confused with other spurious effects such as thixotropy, steric hardening, and viscoelastic short-term recovery of modulus [10, 11]. Thixotropy in asphalt binder has been linked to the softening and decrease in stiffness that is observed during cyclic fatigue tests and the recovery of stiffness during rest periods [12].

Principles of Induction Heating

Induction heating is defined as the process of heating an electrically conductive material using electromagnetic induction [13]. This phenomenon is based on Eddy currents, which are generated when an alternating current is applied to the conductor, such as copper wire, a magnetic field develops in and around the conductor and vice versa [14]. The benefits of induction heating are that the heating process occurs rapidly and no contact is required with the surface; however, the depth of penetration usually drops quickly away from the surface.

Induction heating (IH) is a fast, efficient, and safe approach for warming conductive materials. The principle of the IH is similar to transformer operation. An alternating current passes through a coil and generates an alternating magnetic field in the area around the coil. This varying magnetic field induces a voltage and consequently current in a secondary

conductor. The conductor is an object that will be heated. As the alternating magnetic field induces voltage in the object, Eddy current flows through the object and causes heat due to the resistance opposing the current. Hysteresis losses in ferromagnetic materials can also generate heat in the system, but for non-ferromagnetic materials, this heat is negligible.

One of the main elements in induction heating is the inductor (coil) that generates the alternating magnetic field. A number of factors affect the magnetic field intensity and generated heat by the coil including the number of turns, the enclosed area by the coil, and the coil operating frequency. Available methods of induction heating used in asphalt healing applications utilize high current bars and copper coil that create magnetic fields. The resultant time-varying magnetic field in turn, induces voltage in small metal particles in the asphalt and produces heat in them for healing purposes. This approach requires high currents and long conducting bars to create magnetic field that is strong enough for induction heating inside asphalt.

By contrast, high frequency resonant convertors can be used to create high-frequency low currents in an inductor leading to a time-variable magnetic flux with the same frequency. Such a magnetic field can induce voltage in pieces of metals that are inside or in the close vicinity of the inductor. The efficiency of induction heating and the amount of heat produced by this method rely on a well-tuned circuitry where the conductive elements (metal pieces in the asphalt) play a role in it. Moreover, the range of effectiveness of this method is small as opposed to the former method and thus it can heat up pieces that are very close or in the center of the heating coil (inductor).

Applications of Induction Heating to Asphaltic Materials

While healing is an intrinsic property of asphalt binder, it is practically impossible to grasp the benefits of this characteristic in the field as the flow of traffic is beyond the designer's control. Yet, recent investigations have attempted to accelerate the healing of asphaltic materials by adding conductive materials in the asphalt mixture. A number of studies conducted in Europe have attempted to take advantage of induction heating in accelerating healing mechanisms in asphaltic materials [15, 16]. When conductive asphalt concrete samples are heated electrically, the heat generated through the induction heating mechanism can influence the asphalt mastic resulting in partial or complete healing of the damaged section of the mixture, see Figure 6.

While the approach appears promising, the effectiveness of healing through induction heating is yet to be demonstrated as many influencing variables such as heating time, frequency of the current, magnetic permeability, depth of penetration, may prevent the healing process to take place. Furthermore, limited studies have been conducted to study the recovery of

cracking damage and fatigue resistance properties after healing, which can validate the overall effectiveness of this approach.



Figure 6
Principles of healing through induction heating [16, 17, 18]

A review of the literature shows that researchers have mostly focused on evaluating the effects of steel fibers on the electrical resistivity and induction heating speed in porous asphalt concrete. Liu et al. (2010) showed that induction heating can be used to heat conductive porous asphalt concrete. Steel wool of type 000 and steel fibers of type 1 were used in the porous asphalt concrete samples to make them electrically conductive [17]. Effects of these fibers on electrical resistivity, indirect tensile strength (ITS), and induction heating were tested on asphalt concrete samples with different volume of fibers. From the electrical resistivity test, it was concluded that the samples with lower percentage of fibers showed higher resistivity and samples with steel wool type 000 showed better conductivity. Results showed that ITS value increased with the increase in volume of fibers until an optimum volume of fibers after which ITS value decreased because of reduction in asphalt mastic thickness with the increase in fibers. From the induction heating test, authors have concluded that induction heating temperature is related to electrical resistivity and ITS values of the samples. Furthermore, the samples with optimum content of fibers coinciding with ITS and resistivity tests showed faster heating rates. Finally, it was concluded that induction heating increased the heating rate in conductive porous asphalt concrete and 10% volume of steel wool type 000 was considered as optimum values to be used in asphalt concrete samples to obtain superior results.

Garcia et al. (2011) studied the effectiveness of induction heating on asphalt binder with different volumes of electrically conductive particles and sand-bitumen ratios [18]. Induction heating test was conducted to examine the effect of fiber volume content in the samples; steel wool, of type 000, with diameters between 0.00635 mm and 0.00889 mm were used. Gel-Permeation Chromatography (GPC) method was used to analyze the changes in molecular weight distribution of asphalt concrete samples due to induction heating. The

results from induction heating test indicated that electrical conductivity of the mastic increased with the increase in fiber volume content; however, the addition of more fibers after a certain point (where the temperature does not increase anymore) did not affect the conductivity, see Figure 7. Furthermore, it was observed that addition of more fibers in the asphalt concrete could result in the formation of clusters. Results from chromatographic tests suggested that that induction heating did not change the molecular weight distribution in the samples. Garcia et al. (2011) also evaluated healing effectiveness by breaking and healing the samples repeatedly at low and high temperatures. Results from the stress-strain curves before and after healing indicated the medium resistance of the samples to be about 90% of the original sample and 70% of the original resistance after five cycles of healing. Based on these results, it was concluded that there is an optimum volume of conductive fibers in the mixture above or below which the electrical resistivity remains constant or drops to that of a non-conductive material.

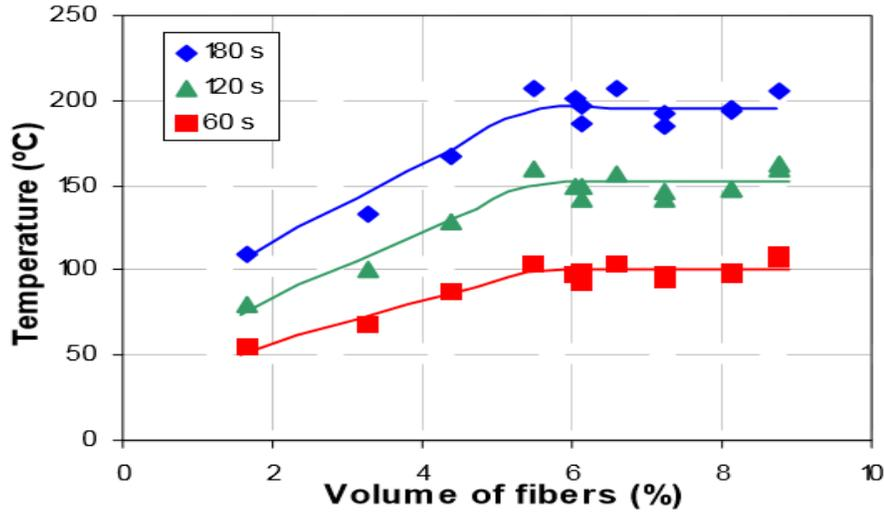


Figure 7
Maximum reachable temperatures at three different heating times for different volume of fibers [18]

Garcia et al. (2012) used an Arrhenius equation and equations derived from various induction heating mechanisms such as thermal capacity, thermal radiation, convection heat and conduction heat to develop a model to study the induction heating times required to achieve complete healing of cracks in asphalt concrete [15]:

$$C' = D * B' (h) - A' T_{air}^4 - B' T_{air} \quad (2)$$

where,

$$A' = \frac{\varepsilon \sigma A_r}{C_{th}}, B' = \frac{h_c A_r}{C_{th}}, D = \frac{\pi r^4 L \mu_m B_r \omega^2}{16 \rho C_{th}} - \frac{\varepsilon \sigma A_r T_{air}^4}{C_{th}} - \frac{h_c A_r T_{air}}{C_{th}}$$

By examining the parameters of the equation derived, the authors have inferred that, parameters A' and B' depends on the intrinsic properties of the material and parameter C' depends on the properties of induction heating machine used, electrical characteristics of the mixture, and on the testing temperature. From these results, it was observed that heat gains and heat losses are two main factors affecting induction heating of which heat gains rely mainly on the radius of the fibers and on their volume in the mixture.

Garcia et al. (2009) conducted an experiment to evaluate the optimum volume of conductive fibers in the asphalt mixture [19]. Porous asphalt mixture was used along with steel wool of type 00 as conductive material in the mixture. Various samples with diameter of 100 mm and varying thickness between 60.62 and 66.45 mm were prepared using three different modes; 2%, 4%, & 6% of fibers were added in first preparation mode and 4% fibers were added in second and third preparation mode. The asphalt mixtures in the first mode were prepared with two different mixing times of 1.5 minute with 3.5 minute. The second mode of preparation was performed in a continuous asphalt plant by using two ways; firstly, the conductive fibers were mixed with bitumen before adding the aggregates and secondly, the fibers were added to the asphalt mixture. In the third mode, fibers were premixed with bitumen and aggregates were added later. These modes of preparation were adopted in order to validate the lab compacted specimens and field cored samples. Indirect tensile test conducted on the lab prepared samples indicated that the volume of fibers and mixing time does not affect the mechanical resistance of the asphalt mixture; the results were observed to be similar with plant mixed and field cored samples. The mixtures with 2% steel fibers with 1.5 or 3.5 minutes of mixing time and 4% steel fibers with 3.5 minutes mixing time were observed to resist the development of clusters as indicated by CT-scanning. The mixing time, length and diameter of the fibers were concluded to have a significant effect on the clusters formation and temperature of induction heating in the asphalt mixtures.

Liu et al. (2013) evaluated the induction healing mechanism of steel-wool reinforced porous asphalt concrete using bending fracture tests on elastic foundation [17]. Bending fracture tests were conducted on porous asphalt beams (50 x 50 x 450mm) prepared with 4% steel wool of type 00 and 5.2% bitumen by weight of the aggregates. The notched beam specimen was placed on an elastic foundation setup, which was developed in order to prevent permanent deformation during the test and close the cracks during unloading. The test procedure consisted of, (1) fracturing of specimen at 5°C with a displacement loading speed of 50 mm/min, (2) heating of fractured specimen with induction heating, and (3) fracturing of healed beam on elastic foundation at same displacement loading speed. Fatigue life extension test was conducted at different temperatures (30, 50, 70, 85, and 100°C) to investigate the effect of low, medium, and high temperatures on healing rate; higher healing rate was achieved at 85°C and further heating resulted on swelling and drainage problems.

At this temperature, the asphalt concrete beam was observed to have the highest strength recovery. Figure 8 presents the strength recovery ratios at different healing temperatures. The authors observed that reheating of the samples does not decrease the strength recovery characteristics of the mix; i.e., the mix can be reheated if the cracks reappear. Furthermore, the cyclic fracturing-healing does not accumulate the damage in the samples.

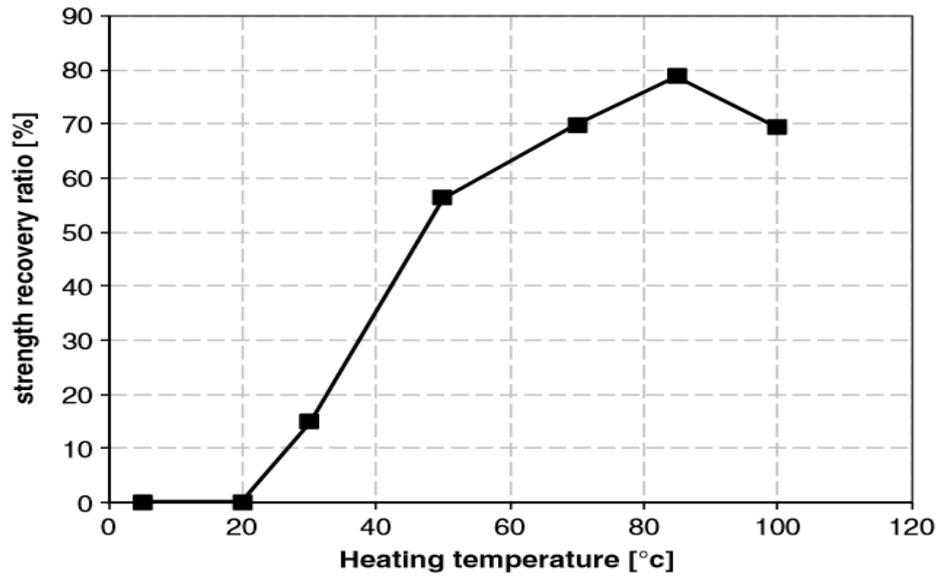


Figure 8
Strength recovery ratios at different healing temperatures [17]

Garcia et al. (2013) studied the effect of steel wool fibers on the porosity and electrical conductivity of dense asphalt concrete [18]. A total of 25 different types of mixtures of same aggregates gradation and bitumen content were prepared using steel wool fibers (type 1, type 3, type 00, and type 000), with four different percentages (0%, 2%, 4%, and 6%), and with two different lengths (short fibers with average length of 2.5 mm and long fibers with average length of 7 mm). The microstructure of asphalt concrete with the addition of different volumes and length of fibers was studied using X-ray microtomography. The length of fibers after compaction was observed to be independent of the initial length as they suffer shear and tension stresses and impacts during the mixing and compaction process, see Figure 9. Fibers were observed to cluster during the initial phase of mixing and grow with the increase in amount and decrease in diameter of the fibers. The authors did not observe any improvement in the flexural strength and particle loss of the asphalt mixture due to the addition of steel wools. The addition of higher percentage of fibers was observed to increase the air void content, which in turn increased the particle loss resistance of the asphalt mixture; however, this increase in particle loss resistance was not significantly higher than

that of the mixture without steel wool fibers. The authors concluded that a uniform distribution of fibers on asphalt mixtures can be achieved if fibers of shorter length and larger diameter are used; addition of 6% or higher volume of fibers with a minimum diameter of 0.15498 mm (type 3) can be added for better distribution and to obtain higher induction heating rates.

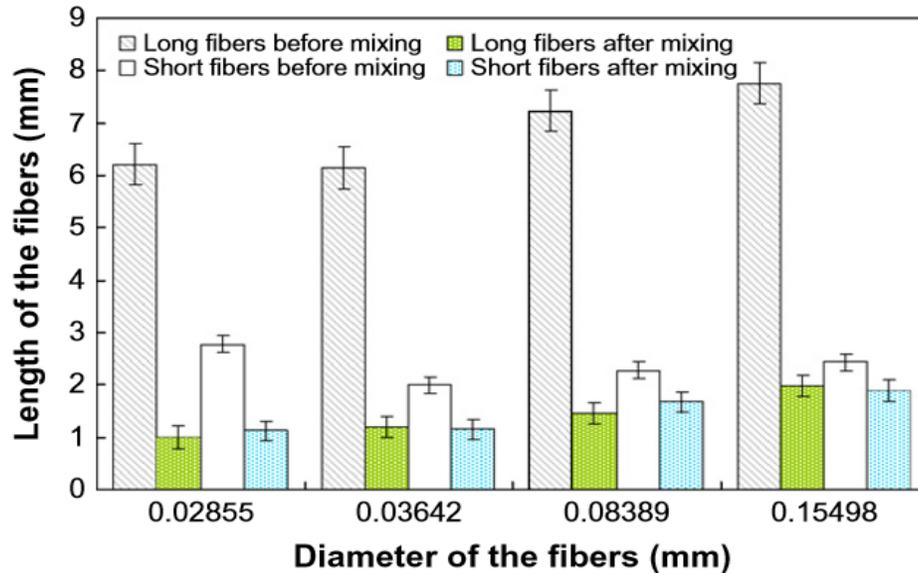


Figure 9
Average length of fibers before and after mixing and compacting [18]

Healing of Cracks through Induction Heating

Garcia et al. (2011) explained self-heating behavior of asphalt mastic with conductive fibers using Arrhenius equation [18]. The required apparent activation energy was calculated by breaking and healing asphalt mastic beams at different temperatures; activation energy was calculated using the time when the recovery was complete. Steel wool, of type 000 (7.5% by weight of the mixture) was used as the conductive fibers. The test samples were subjected to three-point bending to generate cracks crossing the specimen from the tip of the notch to the load application point. The samples were then heated for a period of time ranging from seconds to hours at different temperatures (15°C, 30°C, 40°C, 50°C, 70°C, 90°C, and 100°C). Finally, the samples were tested again under three point bending to measure the resistance to failure. The healing level of asphalt mastic was quantified by the ratio of ultimate force of the beams before and after healing in the three-point bending test. Result from CT-Scan tests, which were performed to observe the healing process indicated that the healing of asphalt mastic starts from the contact points of the cracked area because of the capillary phenomena; healing was observed to be faster in deeply buried cracks. The healing rate of asphalt mastic was observed to increase with the increase in temperature, however, the

mastic shall be heated for a fixed time and above certain temperature. A linear relationship was observed between the activation energy for capillary flow and the capillary diameter. The authors concluded that Arrhenius equation can be used to predict the healing times of asphalt mastic at different temperatures.

Garcia et al. (2009) analyzed the conductivity of asphalt mastic with the addition of electrically conductive fillers and fibers, namely graphite and wool; steel wool of type 000 was used as conductive fiber and graphite was used as a filler in the asphalt mortar [19]. The behavior of asphalt mastic subjected to induction energy was investigated in more than 120 asphalt mortar specimens with different sand-bitumen ratios and volumes of conductive particles. Additionally, a 3D nano CT-scan reconstruction model technique was used to investigate the distribution of electrically conductive materials. Authors concluded that the effect both parameters, i.e., sand-bitumen ratio and volume of conductive particles cannot be examined individually and there exists an optimum volume of fibers for a sand-bitumen ratio for each mix above or below which the resistivity increases which decreases the conductivity of asphalt motor.

Figure 10 presents the electrical conductivity surface of asphalt mortar depending on the sand-bitumen ratio and on the total volume of conductive additives. Three samples were prepared with different volumes of fibers and fixed sand-bitumen ratio to validate the electrical conductivity; the authors concluded that every mix should be analyzed separately by increasing the volume of fibers to obtain optimum conductivity and by adding small proportions of filler to stabilize the resistivity. The sand-bitumen ratio was concluded to be the key factor in design of the conductive mixtures and for each sand-bitumen ratio there exist an optimum volume of conductive fillers above which the fibers start to cluster in the mixture and below which the mixture becomes non-conductive.

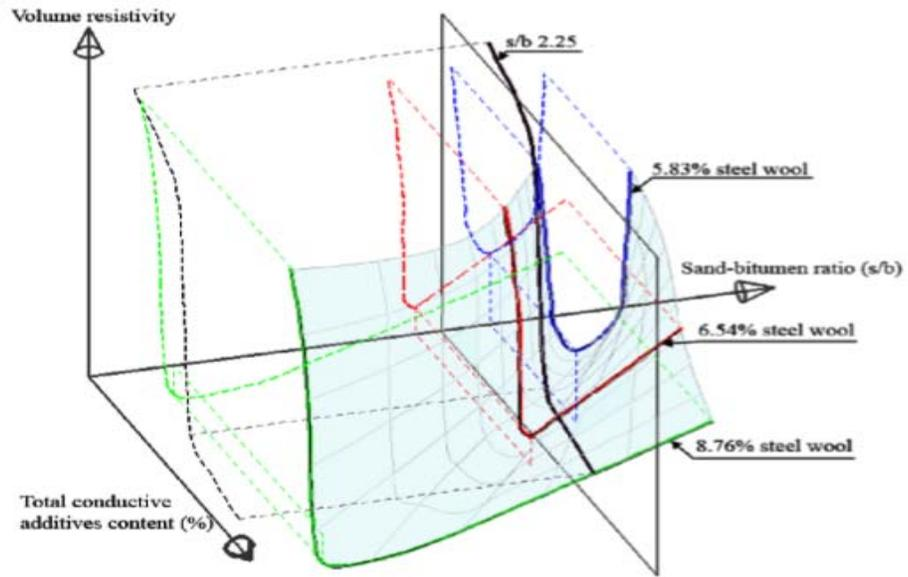


Figure 10
Electrical conductivity surface of asphalt mastic against the sand-bitumen ratio and the total volume of conductive additives [19]

Laboratory Test Results

Job-Mix Formula

Table 2 presents the job mix formula for the prepared OGFC mixes. As shown in this table, the binder content was kept constant in all mixes while a slight reduction in fine content was necessary to accommodate the metallic fibers content in the mix. The air voids content was slightly below the target air voids for OGFC, which usually ranges from 18 to 24%. However, it was comparable between the different mixtures. The AC content met the minimum requirement of 6.5% for this type of mixtures.

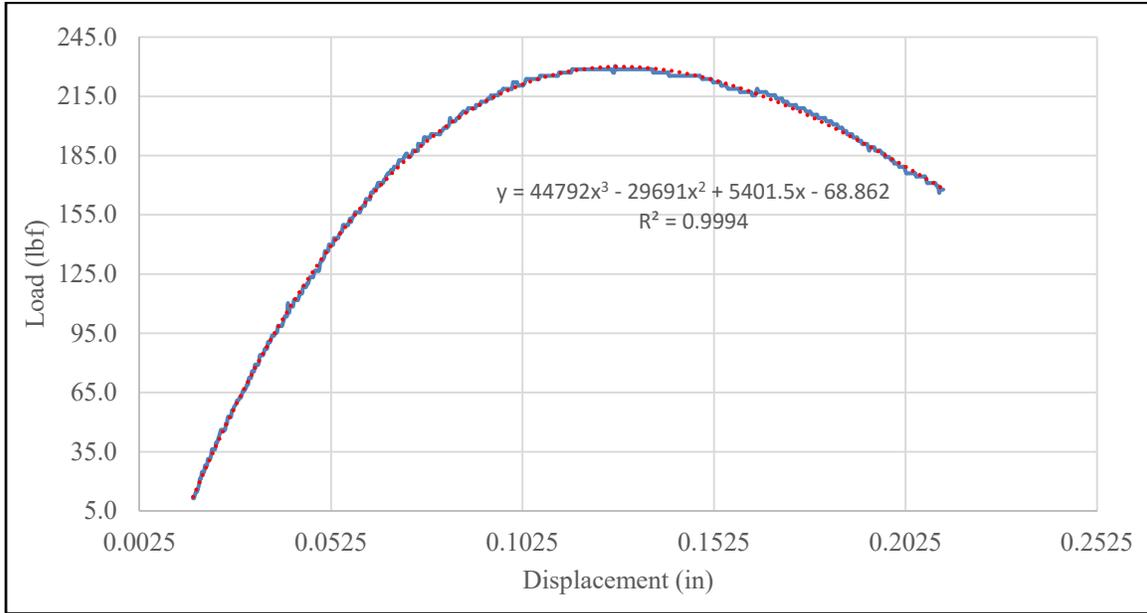
Table 2
Description of the Job Mix Formula

| Parameter | Mixture ID | | | |
|-----------|------------|----------|----------|----------|
| | 76CO | 76Fe2.5% | 76Fe5.0% | 76A15.0% |
| G_{mm} | 2.436 | 2.436 | 2.436 | 2.436 |
| G_{sb} | 2.039 | 2.014 | 2.021 | 2.002 |
| V_a [%] | 16.3 | 17.4 | 17.1 | 17.8 |
| Total %AC | 6.5 | 6.5 | 6.5 | 6.5 |
| 19.0 mm | 100 | 100 | 100 | 100 |
| 12.5 mm | 93.19 | 93.17 | 93.45 | 93.26 |
| 9.5 mm | 71.24 | 71.57 | 71.98 | 72.36 |
| 4.75 mm | 18.01 | 19.24 | 20.31 | 20.36 |
| 2.36 mm | 9.71 | 11.13 | 12.27 | 12.13 |
| 1.18 mm | 8.67 | 10.13 | 11.26 | 11.15 |
| 0.600 mm | 8.35 | 9.83 | 10.98 | 10.94 |
| 0.300 mm | 6.63 | 6.71 | 6.54 | 5.91 |
| 0.150 mm | 5.26 | 5.33 | 5.6 | 5.81 |
| 0.075 mm | 4.10 | 3.88 | 3.52 | 3.77 |

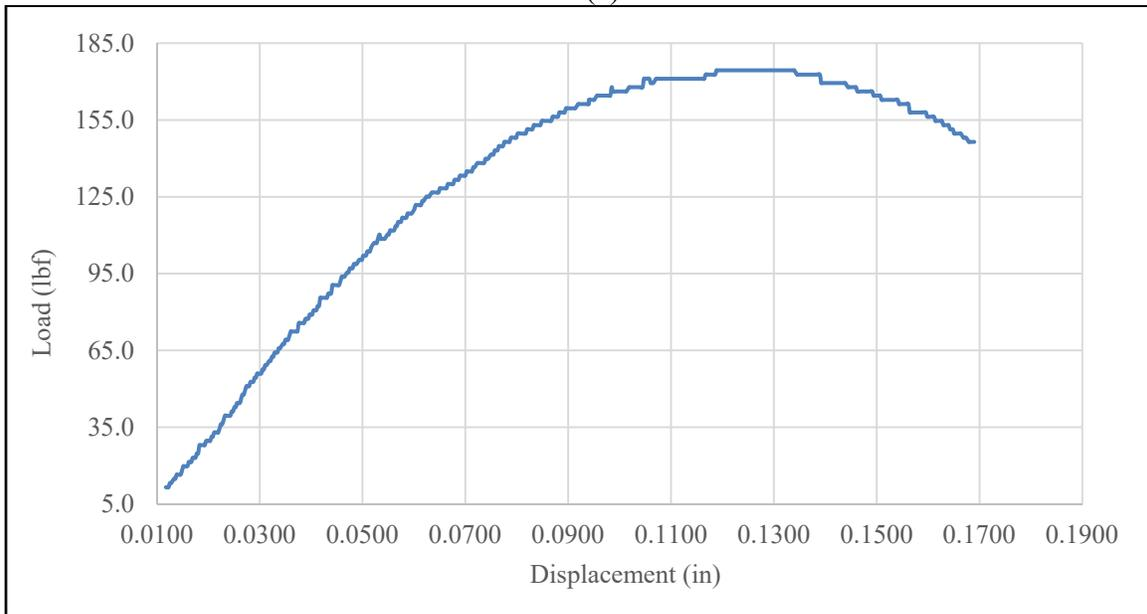
Fracture Resistance of Laboratory Specimens

Figure 11 illustrates typical test results from the fracture resistance test for the control mix and the mix with 5% steel fibers. As shown in this figure, the vertical load applied on the sample gradually increased as the displacement-controlled through the actuator was progressively increased. The specimen resists the applied displacement up to the fracture point and then starts failing; after that, the required load to induce the prescribed displacement gradually decreased until failure of the specimen was reached. To assist in the analysis of the data, polynomial models were fitted to the measurements, see Figure 11a.

While there is no practical use for these models, they allow reducing fluctuation in the measurements and noises in the raw data. The coefficients of determination (R^2) for these models were greater than 0.9 for all cases.



(a)



(b)

Figure 11
Typical Test Results from the Fracture Resistance Test for (a) Control and (b) Mix with 5% Steel Fibers

Table 3 presents the ultimate load and associated displacement for the different mixes evaluated in this study. Repeatability of the measurements was acceptable with a coefficient of variation ranging from 4.8 to 13.2% with an average of 8.0%.

Table 3
Fracture Resistance Test Results before Healing

| Mix ID | Specimen ID | P _{ult} (lb.) | Average P _{ult} (lb.) | Displacement (δ _{ult}) at P _{ult} (in.) | Average δ _{ult} (in.) |
|----------|-------------|------------------------|--------------------------------|--|--------------------------------|
| 76CO | 1 | 230.3 | 210.6 | 0.1267 | 0.1422 |
| | 2 | 190.9 | | 0.1577 | |
| 76Fe2.5% | 1 | 181.0 | 170.3 | 0.1993 | 0.1994 |
| | 2 | 159.6 | | 0.1995 | |
| 76Fe5.0% | 1 | 174.4 | 181.8 | 0.1340 | 0.1233 |
| | 2 | 189.2 | | 0.1126 | |
| 76Al5.0% | 1 | 222.1 | 214.7 | 0.1230 | 0.1219 |
| | 2 | 207.3 | | 0.1207 | |

Figure 12 illustrates a comparison of the mean ultimate load for the conventional and mixes with metallic fibers prior to healing. The conventional mixture was compared to the mixtures prepared with metallic fibers using a t-test with 95% confidence level ($\alpha=0.05$). The letters displayed in the figure represent the statistical grouping associated with the ultimate load. As shown in this figure, while the control mix (76CO) and the mix prepared with aluminum (76Al5.0%) exhibited greater ultimate load at failure than the specimens with steel fibers, the differences were not statistically significant as evident by the letter A assigned to the different mixes.

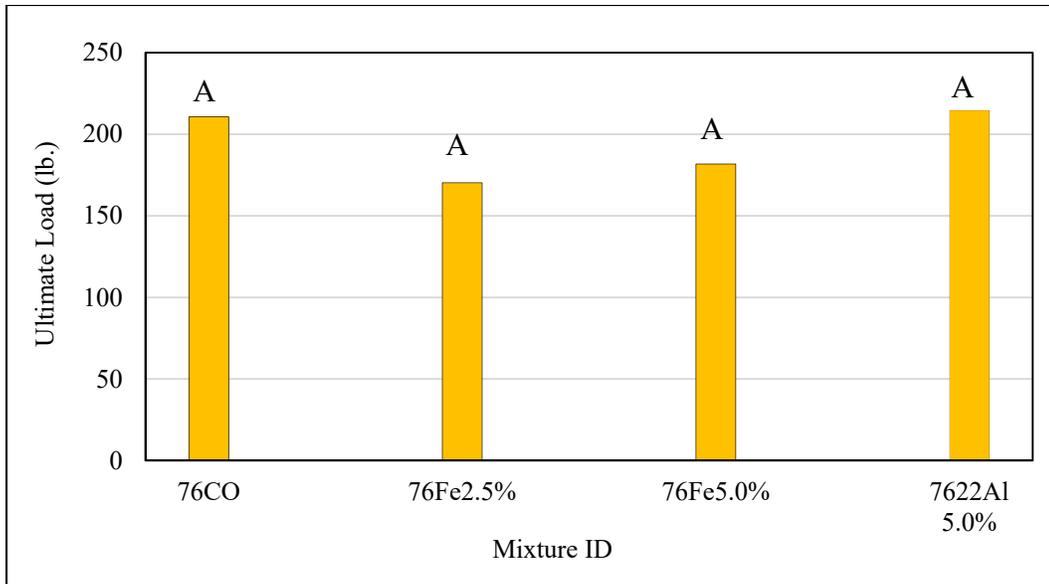


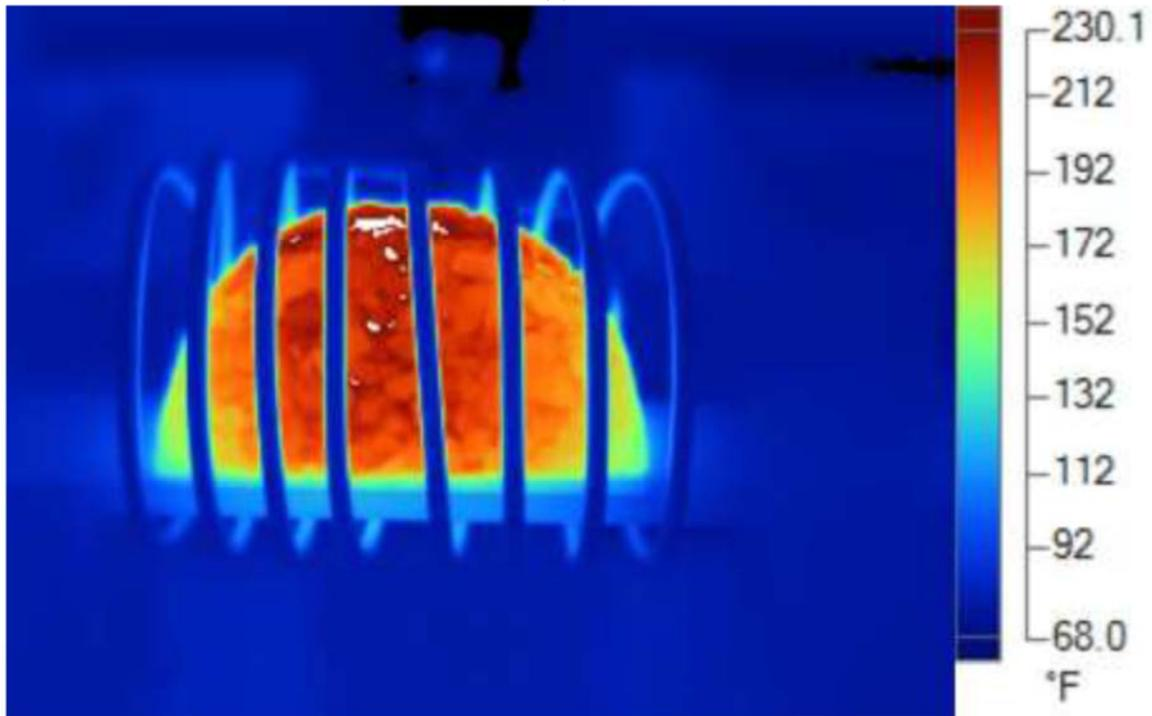
Figure 12
Fracture Resistance Test Results prior to Healing

Healing through Induction Heating

Laboratory specimens were subjected to induction heating until the specimens reached a surface temperature of 110°C (230°F). Induction heating experiments were conducted at the Ambrell Corporation in New York. In this experiment, an alternating current was passed through a coil and generated an alternating magnetic field in the area around the coil. This varying magnetic field induced a voltage and consequently current in the metallic fibers inside the specimen. As the alternating magnetic field induced voltage in the specimen, Eddy current flows through the metallic fibers and caused heat due to the resistance opposing the current. Figure 13 compares the thermal profiles of two specimens, one with 5.0% steel fibers and a control specimen with no metallic fibers after 15 minutes of induction heating. As shown in this figure, the control specimen did not heat throughout the experiment while kept under a magnetic field for 35 minutes. In contrast, the specimen with 5.0% steel fibers reached the target temperature after only 10 minutes.



(a) 76CO



(b) 76Fe5.0

Figure 13
Thermal Profiles of Laboratory Specimens after 15 minutes for (a) 76CO and (b) 76Fe5.0

Table 4 presents the required heating time for each laboratory specimen to reach a temperature of 110°C. It is noted that the temperature measuring interval was set at five minutes in the experiment, which explain why the specimens with 2.5 and 5.0% steel fibers required a comparable induction heating time to reach 110°C. It was also observed that while the specimens with aluminum successfully heated, they required a longer heating time to reach 110°C. This may due to the fact that the electrical resistivity of aluminum is $2.82 \times 10^{-8} \Omega.m$ at 20°C while the electrical resistivity of steel is $6.90 \times 10^{-7} \Omega.m$, which would allow faster heating of the specimen at the same fiber content.

Table 4
Laboratory Induction Heating Time to Reach Target Temperature

| Mix ID | Specimen ID | Induction Time (minutes) |
|---------|-------------|--------------------------|
| 76CO | 1 | Did not heat |
| | 2 | Did not heat |
| 76Fe2.5 | 1 | 10 |
| | 2 | 10 |
| 76Fe5.0 | 1 | 10 |
| | 2 | 10 |
| 76Al5.0 | 1 | 35 |
| | 2 | 30 |

Healing Quantification

After the induction heating experiment, specimens were loaded once more monotonically until failure using the semi-circular bending test setup. It is worth noting that some specimens were damaged during the induction heating experiment due to excessive heat and could not be tested after healing. The recovery period between the first loading stage and the second loading stage was 14 days. Table 5 presents the measured ultimate load and terminal displacement for each specimen type after the induction heating experiment.

Table 5
Fracture Resistance Test Results after Healing

| Mix ID | Specimen ID | P _{ult} (lb.) | Average P _{ult} (lb.) | Displacement (δ _{ult}) at P _{ult} (in.) | Average δ _{ult} (in.) |
|----------|-------------|------------------------|--------------------------------|--|--------------------------------|
| 76CO | 1 | 179.3 | 176.9 | 0.1387 | 0.1221 |
| | 2 | 174.4 | | 0.1055 | |
| 76Fe2.5% | 1 | N/A | - | N/A | - |
| | 2 | N/A | | N/A | |
| 76Fe5.0% | 1 | 113.5 | 113.5 | 0.1066 | 0.1066 |
| | 2 | N/A | | N/A | |
| 76Al5.0% | 1 | 154.7 | 154.7 | 0.1815 | 0.1815 |
| | 2 | N/A | | N/A | |

Figure 14 illustrates a comparison of the mean ultimate load for the conventional and modified mixes after healing. The conventional mixture was compared to mixture prepared with metallic fibers using a t-test with 95% confidence level ($\alpha=0.05$). The letters displayed in the figure represent the statistical grouping associated with the ultimate load. As shown in this figure, while the control mix (76CO) and the mix prepared with aluminum (76Al5.0%) appeared to exhibit greater ultimate load at failure than the specimens with steel fibers, the differences were not statistically significant.

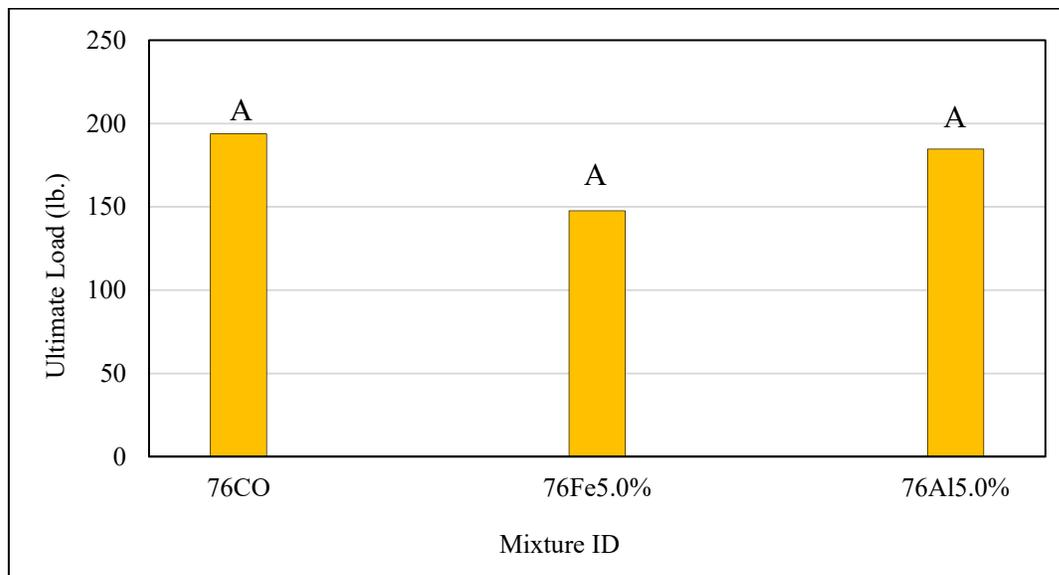


Figure 14
Fracture Resistance Test Results after Healing

Figure 15 illustrates a comparison between the ultimate load before and after healing. It is interesting to note that the control mix had the highest ultimate load after healing although it was not successfully heated through Eddy current as shown in Table 4. This indicates that other healing mechanisms were present due to the long recovery period, which allowed the control specimen to heal during the rest period.

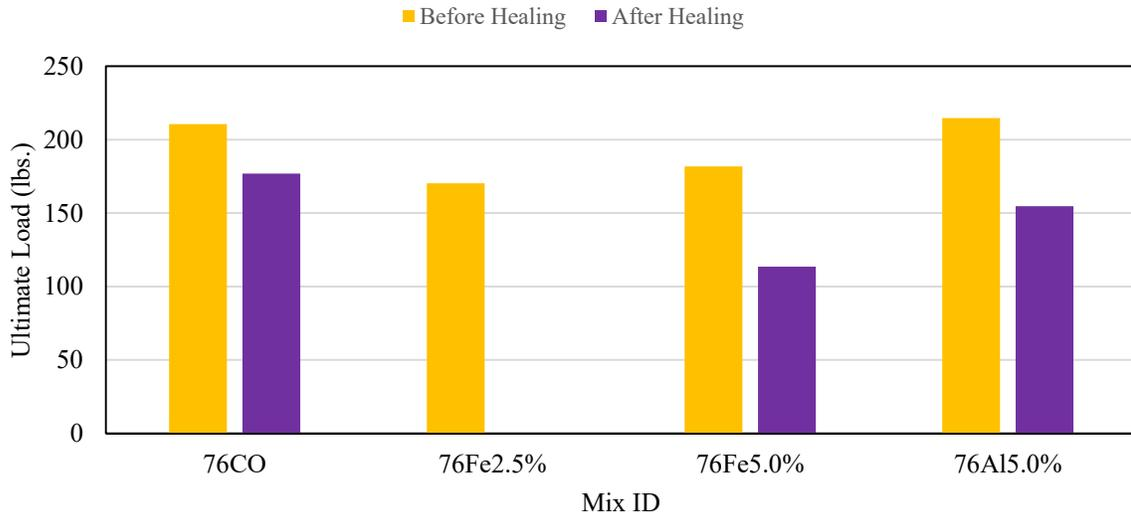


Figure 15
Comparison of the ultimate load before and after the induction heating experiment

To quantify healing efficiency, measured ultimate loads before and after healing were used to estimate the healing efficiency as follows:

$$\text{Healing Efficiency (\%)} = \frac{P_{\text{ult after healing}}}{P_{\text{ult before healing}}} \times 100 \quad (1)$$

where,

$P_{\text{ult after healing}}$ = measured ultimate load of the damaged specimen after healing; and

$P_{\text{ult before healing}}$ = measured ultimate load of the specimen before healing.

Based on Equation (1), a specimen would exhibit 100% healing efficiency if the fracture failure load is recovered entirely after the healing phase. Figure 16 presents the calculated healing efficiency for the different specimen types. Results presented in this figure show that the control specimen exhibited the maximum healing efficiency, which approached 85%.

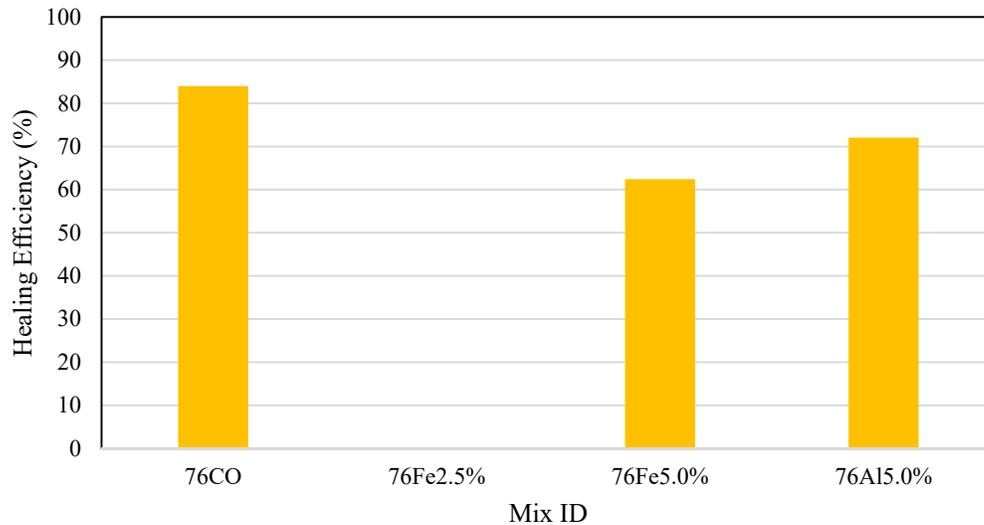


Figure 16
Calculated Healing Efficiency for the Different Mix Types

Microscopic Analysis

Before and after healing the semi-circular specimens, light microscopy images of selected locations were acquired to compare the qualitative geometry of the cracked areas. Table 6 presents the captured microscopic images before and after inducing heating and the recovery period. As shown in this table, all specimens exhibited healing of cracked areas including the control specimens. For the control specimens, cracks with width as large as 0.639 mm appeared to have completely closed after the recovery period. The observed healing of the cracks is in agreement with the measured loading capacity of the specimens after the recovery period.

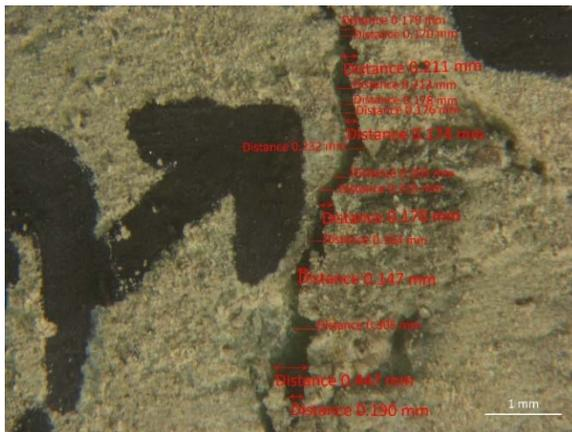
Table 6
Microscopic Images of Cracked Areas after Loading and after the Recovery Period



76CO: Control Mix



76Fe5.0%: Mix with 5% Steel Fibers



76Al5.0%: Mix with 5% Aluminum

Figure 17 compares the measured crack widths before and after induction heating (IH) as determined from digital image analysis using ZEN Digital Imaging software 2.0. The healing efficiency for each mix type based on digital image analysis is presented on top of the columns after healing. As shown in this figure, the control mix showed the highest level of healing efficiency, followed by the mix with aluminum fibers, and finally the mix with steel fibers. The inferior performance of the mix with steel fibers may be due to poor bonding between the steel fibers and the asphalt mixture components. However, further testing would be needed to confirm this assumption.

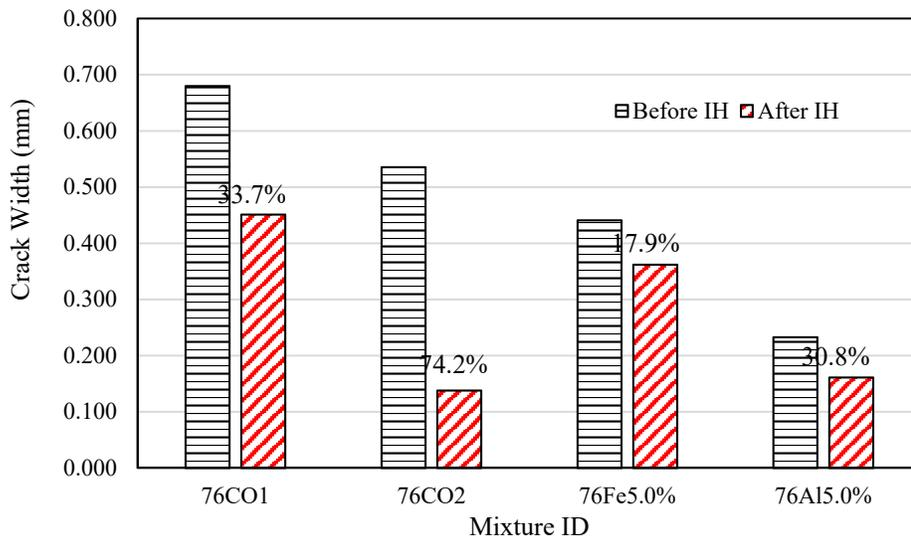


Figure 17
Measured Crack Widths for the Different Mix Types (before and after Induction Heating)

CONCLUSIONS

The objective of this study was to test the hypothesis that a new generation of asphaltic materials could be artificially healed while in-service by embedding metallic fibers in the mix and by applying a magnetic field at the surface. If successful, self-healing through induction heating will result in a new class of asphaltic materials that is able to resist cracking propagation and damage, which is the main failure mechanism in flexible pavements. During the experimental program, an open-graded friction course was successfully designed and prepared to incorporate up to 5% steel and aluminum fibers by weight of the mix. The repeatability of the fracture resistance measurements was acceptable with a coefficient of variation ranging from 4.8 to 13.2% with an average of 8.0%. Based on the results of the experimental program, the following conclusions may be drawn:

- Prior to healing, the control mix and the mix prepared with aluminum fibers exhibited greater ultimate load at failure than the specimens with steel fibers. Yet, differences were not statistically significant.
- The induction heating experiment was conducted successfully and showed the feasibility of inducing Eddy current in the metallic fibers without contact to the specimens. Eddy current flowed through the metallic fibers and caused heat due to the resistance opposing the current.
- Induction heating experiments showed that the specimens incorporating metallic fibers reached the target temperature while the control mix did not heat after 35 minutes. Given their higher electrical resistivity, the specimens with aluminum required a longer heating time to reach 110°C than the specimens with steel fibers.
- After the rest period, the control mix had the highest ultimate load after healing although it was not successfully heated through Eddy current; yet, differences were not statistically significant. This indicates that other healing mechanisms were present due to the long recovery period, which allowed the control specimen to heal during the rest period.
- Healing efficiency was the highest for the control specimen as it approached 85%. Healing efficiency for the specimen with aluminum and steel fibers was 72 and 62%, respectively.
- Microscopic image analysis demonstrated that induced cracks healed efficiently during the healing period. From the captured images, cracks with width as large as 0.639 mm appeared to have completely closed after the recovery period. The observed healing of the cracks is in agreement with the measured loading capacity of the specimens after the recovery period.

RECOMMENDATIONS

Based on the results of the study, asphalt mixture healing through induction heating was validated and is a promising technology. Yet, the conducted experiment was limited in scope and further testing is recommended through a comprehensive testing program. Furthermore, the use of different classes of steel and aluminum fibers will allow to improve the healing efficiency of asphalt specimens through induction heating. The evaluation of healing through induction heating in field applications should also be considered in future projects especially at the Louisiana Accelerated Loading Facility (ALF).

ACRONYMS, ABBREVIATIONS, AND SYMBOLS

| | |
|--------|--|
| AASHTO | American Association of State Highway and Transportation Officials |
| ALF | Accelerated Loading Facility |
| cm | centimeter(s) |
| CT | Computed Tomography |
| FHWA | Federal Highway Administration |
| ft. | foot (feet) |
| in. | inch(es) |
| LADOTD | Louisiana Department of Transportation and Development |
| LTRC | Louisiana Transportation Research Center |
| lb. | pound(s) |
| IH | Induction Heating |
| m | meter(s) |
| OGFC | Open-Graded Friction Course |

REFERENCES

1. Bazin, P., and Saunier, J.B. "Deformability, Fatigue, and Healing Properties of Asphalt Mixes." Proc., 2nd International Conference on the Structural Design of Asphalt Pavements, University of Michigan, Ann Arbor, MI, 1967, pp. 553-569.
2. Van Dijk, W., Moreaud, H., Quedeville, A., and Uge, P. "The Fatigue of Bitumen and Bituminous Mixes." Proc., 3rd International Conference on the Structural Design of Asphalt Pavements, University of Michigan, Ann Arbor, MI, 1972, pp. 354-366.
3. Carpenter, S.H., and Shen, S. "A Dissipated Energy Approach to Study Hot-Mix Asphalt Healing in Fatigue." In Transportation Research Record 1970. Transportation Research Board, National Research Council, Washington, D.C., 2006.
4. Palvadi, S., Bhasin, A., and Little, D.N. "A Method to Quantify Healing in Asphalt Composites Using Continuum Damage Approach." In Transportation Research Record 2296, Transportation Research Board, National Research Council, Washington, D.C., 2012, pp 86-96.
5. Qiu, J., van de Ven, M.F.C., Wu, S.P., Yu, J.Y., and Molenaar, A.A.A. "Investigating Self-Healing Behavior of Pure Bitumen Using Dynamic Shear Rheometer." Fuel (90), 2011, pp. 2710-2720.
6. Phillips, M.C. "Multi-Step Models for Fatigue and Healing, and Binder Properties Involved in Healing." Eurobitume workshop on performance-related properties for Bituminous Binders, European Bitumen Association, Luxembourg, 115, 1998.
7. Kim, Y.R. "Evaluation of Healing and Constitutive Modeling of Asphalt Concrete by Means of the Theory of Nonlinear Viscoelasticity and Damage Mechanics." PhD in Civil Engineering, Texas A&M University, College Station, 1988.
8. Qiu, J., van de Ven, M., and Molenaar, A.A.A. "Crack Healing Investigation in Bituminous Materials." ASCE Journal of Materials in Civil Engineering, Vol. 25, No. 7, 2013, pp. 864-870.
9. Wool, R.P., and O'Connor, K.M. "A Theory Crack Healing in Polymers". Journal of applied physics, volume 52 (10), 1981, pp. 5953-5963.
10. Santagata, E., Baglieri, O., Tsantilis, L., Dalmazzo, D. "Evaluation of Self-Healing Properties of Bituminous Binders Taking into Account Steric Hardening Effects." Construction and Building Materials, Vol. 41, 2013, pp. 60-67.

11. Shen, S., and Lu, X. "Fracture Healing Properties of Asphaltic Material Under Controlled Damage." ASCE, Journal of Materials in Civil Engineering, Vol. 26, No. 2, 2014, pp. 275-282.
12. Shan, L., Tan, Y., Underwood, B.S., and Kim, Y.R. "Thixotropic Characteristics of Asphalt Binder." ASCE, Journal of Materials in Civil Engineering, Vol. 23, No. 12, 2011, pp. 1681-1686.
13. Valery, R. "Handbook of Induction Heating." CRC Press, 2003.
14. Hellier, C.J. "Handbook of Nondestructive Evaluation." 2nd Edition, McGraw Hill, 2013.
15. Garcia, A., Schlangen, E., Ven, M.V., and Liu, Q. "A Simple Model to Define Induction Heating in Asphalt Mastic." Construction and Building Materials, Vol. 31, 2012, pp. 38-46.
16. Liu, Q., Schlangen, E., Garcia, A., Ven, M.V., and Poot, M. "Optimization of Steel Fiber used for Induction Heating in Porous Asphalt Concrete." Traffic and Transportation Studies, ASCE, 2010, pp. 1320-1330.
17. Liu, Q., Schlangen, E., Garcia, A., and Ven, M.V. "Induction Heating of Electrically Conductive Porous Asphalt Concrete." Construction and Building Materials, Vol. 24, 2010, 1207-1213.
18. Garcia A., Schlangen, E., Ven, M.V., and Viet, D.V. "Crack Repair of Asphalt Concrete with Induction Energy." HERON, Vol. 56, 2011, 34-43.
19. Garcia, A., Schlangen, E., Van de Ven, M., and Liu, Q. "Electrical Conductivity of Asphalt Mortar Containing Conductive Fibers and Fillers. Construction and building materials, 23(10), 2009, pp. 3175-3181.